analytical chemistry

Article

pubs.acs.org/ac

Simultaneous Detection of Nonpolar and Polar Compounds by Heat-Assisted Laser Ablation Electrospray Ionization Mass Spectrometry

Anu Vaikkinen,[†,‡] Bindesh Shrestha,[‡] Javad Nazarian,[§,⊥] Risto Kostiainen,[†] Akos Vertes,*[,‡] and Tiina J. Kauppila*[,†]

[†]Division of Pharmaceutical Chemistry, Faculty of Pharmacy, P.O. Box 56, 00014, University of Helsinki, Finland

[‡]Department of Chemistry, W. M. Keck Institute for Proteomics Technology and Applications, George Washington University, Washington, D.C. 20052, United States

[§]Research Center for Genetic Medicine, Children's National Medical Center, Washington, D.C. 20010, United States

[⊥]Department of Integrative Systems Biology, School of Medicine and Health Sciences, George Washington University, Washington, D.C. 20037, United States

Supporting Information

ABSTRACT: A heat-assisted laser ablation electrospray ionization (HA-LAESI) method for the simultaneous mass spectrometric analysis of nonpolar and polar analytes was developed. The sample was introduced using mid-infrared laser ablation of a water-rich target. The ablated analytes were ionized with an electrospray plume, which was intercepted by a heated nitrogen gas jet that enhanced the ionization of analytes of low polarity. The feasibility of HA-LAESI was tested by analyzing, e.g., naphtho[2,3-*a*]pyrene, cholesterol, tricaprylin, 1,1′,2,2′-tetramyristoyl cardiolipin, bradykinin fragment 1−8, and 1-palmitoyl-2-oleoyl-*sn*-glycerol. HA-LAESI was found better suited for low polarity compounds than conventional LAESI, whereas polar compounds were observed with both techniques. The sensitivity of HA-LAESI for the polar bradykinin fragment 1−8 was slightly lower than observed for LAESI. HA-LAESI showed a linear response for 500 nM to 1.0 mM solutions (n = 11) of verapamil with R^2 = 0.988. HA-LAESI was applied for the direct analysis of tissue samples, e.g., avocado (*Persea americana*) mesocarp and mouse brain tissue sections. Spectra of the avocado showed abundant triglyceride ion peaks, and the results for the mouse brain sections showed cholesterol as the main species. Conventional LAESI shows significantly lower ionization efficiency for these neutral lipids. HA-LAESI can be applied to the analysis of nonpolar and polar analytes, and it extends the capabilities of conventional LAESI to nonpolar and neutral compounds.

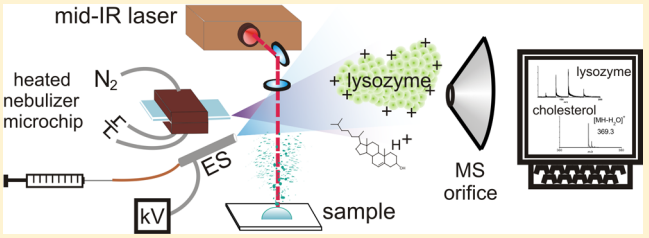

Ambient mass spectrometry (MS)[1,2] is a young family of techniques for direct, local analysis of complex samples. The sample can be analyzed in its native state, while the analytes are desorbed and ionized directly from the sample surface. Ambient MS speeds up analyses, and facilitates in situ and in vivo experiments, because the conventional sample preparation and separation before the MS analysis are omitted. Ambient MS also provides new tools for molecular imaging of surfaces.[3] Ambient MS techniques with sufficient lateral resolution can even make possible biological analyses at the single cell level.[4] Ambient MS was preceded by techniques such as matrix-assisted laser desorption/ionization (MALDI),[5] and secondary ion mass spectrometry (SIMS), which can be utilized in similar surface analyses. MALDI and SIMS have excellent lateral sampling resolutions starting from ∼600 nm[6] and 50 nm,[7] respectively, that have not yet been achieved with ambient MS. MALDI has become an established tool in bioanalysis, especially in proteomics, while SIMS is in wide use in trace element detection from, for example, semiconductors. However, in both SIMS and traditional MALDI the analysis takes place in a vacuum environment, which can compromise the integrity of biological samples, such as cells that burst in vacuum, and also limits the feasibility of high throughput screening applications. In addition, MALDI requires the application of a chemical additive, a matrix, which causes substantial chemical background at low m/z (<500 amu). Recently the development of surface analysis techniques has shifted toward ambient MS, because they are mostly free of matrix and they take place in open environment so that samples can be rapidly analyzed under conditions more closely resembling those in vivo.

Ambient MS includes methods such as desorption electrospray ionization (DESI),[8] laser ablation electrospray ionization (LAESI),[9] electrospray-assisted laser desorption/ionization (ELDI),[10] matrix-assisted laser desorption electrospray ionization (MALDESI),[11] direct analysis in real time (DART),[12]

Received: August 23, 2012
Accepted: December 3, 2012
Published: December 3, 2012

desorption atmospheric pressure photoionization (DAPPI),[13] and laser ablation atmospheric pressure photoionization (LAAPPI).[14] Electrospray ionization (ESI) based techniques, e.g., DESI,[8] LAESI,[9] ELDI,[10] and MALDESI,[11] are powerful for the surface analysis of polar compounds such as peptides, proteins, and phospholipids. Chemical ionization and photoionization-based techniques such as DART,[12] DAPPI,[13] and LAAPPI[14] provide more sensitive analysis of low polarity compounds, such as steroids and polyaromatic hydrocarbons, but they are limited to relatively small molecules (<1000 amu), because the analytes are desorbed (DART, DAPPI) or desolvated (LAAPPI) by a hot gas stream that fragments thermolabile compounds. A single, more universal ionization technique would be advantageous because of wider coverage of analytes in a single analysis and reduced sample consumption. It would also give more detailed knowledge for complex samples, such as single cells, because instead of using parallel specimens in complementary analyses, data could be obtained from the same sample. Wide ionization range has been previously achieved using dual or multimode ion sources. For example, desorption electrospray/metastable-induced ionization (DEMI)[15] combines DESI- and DART-type sources and has been used to simultaneously analyze, for example, dibromodibenzosuberone and angiotensin I. DESI has also been combined with direct ionization by charge exchange (DICE).[16] The combination of DESI and DICE has been applied to the analysis of, for example, pharmaceutical tablets, and it shows better ionization efficiency for low polarity compounds than DESI alone. While these two techniques are promising, their lateral resolution is expected to be lower than that achieved with laser-based techniques.

Here, we introduce heat-assisted laser ablation electrospray ionization (HA-LAESI), a novel variant of LAESI, which enables the simultaneous analysis of nonpolar and polar analytes of various sizes, and apply it to the analysis of plant and animal tissues. In LAESI, the analytes are ablated from water-rich samples, such as droplets of aqueous liquids or solid biological tissues containing endogenous water, using a mid-IR laser that is focused on the sample surface. The photons rapidly excite the OH bond of water molecules, which leads to superheating, phase explosion, and efficient ablation of the analytes from the surface. With LAESI, finely localized ablation of spots can be achieved with diameters as small as 40−200 μm.[4] The ablation releases sample particulates that are picked up by droplets formed by an orthogonal electrospray. When inside the electrically charged droplets, the analytes are ionized similarly to that for traditional electrospray ionization. Thus far, LAESI has been applied to molecular imaging, single cell, and cell population analyses.[4,9,17,18] It has high ionization efficiency for polar compounds, such as proteins, peptides, and phospholipids, but the ionization efficiency for nonpolar and neutral compounds is lower. A related complementary technique for nonpolar and neutral analytes, called LAAPPI,[14] was recently introduced. LAAPPI uses a krypton discharge lamp for ionization instead of electrospray ionization (ESI) and thus efficiently ionizes nonpolar and neutral molecules, e.g., lipids, but the detection of peptides and proteins by LAAPPI is limited by their fragmentation. Here we show that both polar and nonpolar analytes can be simultaneously ionized by using HA-LAESI. The method is evaluated by analyzing a group of compounds of different sizes and polarities, and it is compared with conventional LAESI and LAAPPI. The novel HA-LAESI technique is also applied to rapid profiling of avocado (*Persea americana*) mesocarp, mouse brain tissue sections, and pansy (*Viola*) petals.

EXPERIMENTAL SECTION

Chemicals and Samples. Water (HPLC grade) and cholesterol (96%) were from Alfa Aesar (Ward Hill, MA), 1-palmitoyl-2-oleoyl-*sn*-glycerol (DG(34:1), 2 mg/mL in chloroform) and 1,1′,2,2′-tetramyristoyl cardiolipin (TMCL) sodium salt were obtained from Avanti Polar Lipids (Alabaster, AL), and methanol (LC-MS grade) and formic acid (~98%) were produced by Fluka (Seelze, Germany). Toluene (HPLC grade, 99.9%), perylene, naphtho[2,3-*a*]pyrene (98%), lysozyme from chicken egg white, fucose (>99%), 1,2-dioleoyl-*sn*-glycero-3-phosphocholine (DOPC), dehydroepiandrosterone (DHEA, ≥99%), verapamil hydrochloride (verapamil, 99%), estrone (99%), cholecalciferol (≥98%), glyceryl trioctanoate (tricaprylin, ≥99%), bradykinin fragment 1−8 acetate hydrate (bradykinin 1−8, peptide content 86%), and pyrene were purchased from Sigma-Aldrich (St. Louis, MO). Nitrogen was obtained via the mass spectrometer nebulizer gas line from a nitrogen tank (refrigerated industrial grade liquid 99.8%, GTS-Welco, Inc., Allentown, PA) and was further regulated by a mass flow controller GFC17 by Aalborg (Orangeburg, NY).

Stock solutions of the analytes were prepared as detailed in Table S1 of the Supporting Information. All sample solutions were prepared in methanol/water (1:1, v:v). Aliquots of 0.5−10 μL were pipetted onto concave microscope glass slides and analyzed as liquid droplets. The electrospray solution was prepared by mixing methanol and water in 1:1 (v:v) ratio and adding 0.1% formic acid by volume. Verapamil was added to the electrospray solution for the analysis of a mouse brain tissue section (final concentration of 25 nM) and avocado mesocarp (40 nM) for internal mass calibration.

Avocado (*Persea americana*) fruits and pansy (*Viola*) plants were obtained from a local supermarket. The avocado was cut with a blade and placed on a microscope glass slide after producing ~10 × 20 × 0.5 mm sections using a manual microtome. The flower petals of the pansy were attached to a glass microscope slide using adhesive tape without any pretreatment. Mouse brain samples were obtained from a healthy BALB/c albino mouse strain from the Jackson Laboratory (Bar Harbor, ME). The mice were euthanized by cervical dislocation at average ages of 11−12 months. All animal procedures and experiments fully complied with the principles set forth in the "Guide for the Care and Use of Laboratory Animals" prepared by the Committee on Care and Use of Laboratory Animals of the Institute of Laboratory Resources, National Research Council, and were approved by the Children's National Medical Center's Institutional Animal Use and Care Committee. Brain specimens were snap-frozen using isopentane cooled in liquid nitrogen and stored at −80 °C. Brain specimens were embedded in Optimal Cutting Temperature (OCT) solution (Sakura Finetek, Torrance, CA) and sectioned using a cryostat set to −25 °C and 40 μm thickness. Brain sections were directly used for mass spectrometric analysis without any pretreatment.

Mass Spectrometry. A JEOL AccuTOF JMS-T100LC mass spectrometer (JEOL Ltd., Peabody, MA) was used for mass analysis. LAESI, heat-assisted LAESI, and LAAPPI ion sources were set up in front of the sampling orifice of the mass spectrometer. The orifice temperature was set to 150 °C and voltage to 20 V. The spectrum acquisition time was set to 1 s.

dx.doi.org/10.1021/ac302432h | *Anal. Chem.* 2013, 85, 177−184

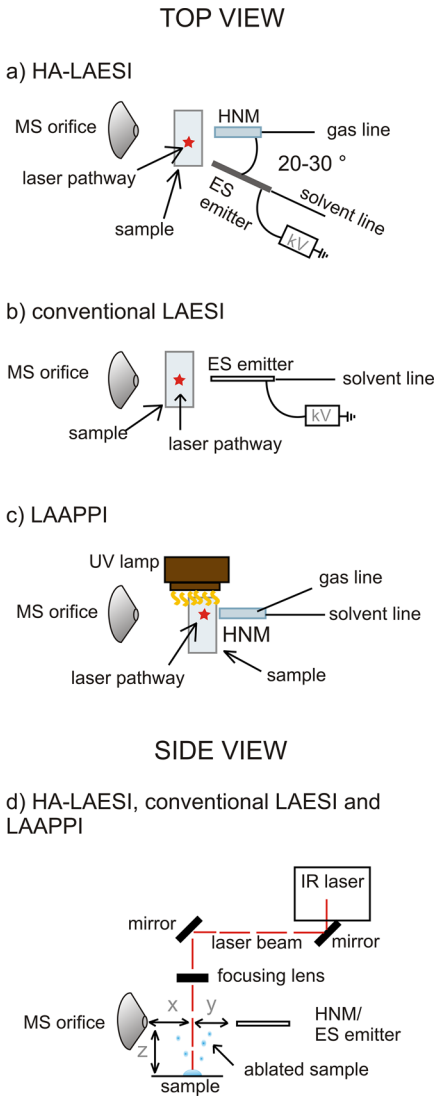

Figure 1. A schematic representation of the (a) HA-LAESI, (b) conventional LAESI, and (c) LAAPPI set-ups (not to scale) seen from the top with the focusing lens and mirror hidden to show the components relevant for the ionization process. The star shows the approximate alignment of the laser pathway in each setup. (d) Representation of all three set-ups seen from the side, showing the introduction of the sample to the ionization area by laser ablation. The heated nebulizer microchip (HNM), the ES emitter, and the UV lamp (not shown in d) were aligned in the same plane as the mass spectrometer inlet. The distance of the sample from the axis of the mass spectrometer orifice (z) was 8−20 mm, whereas x and y were adjusted depending on the ionization method as described in the Experimental Section.

Ion Sources. *LAESI Source with Heated Gas Flow.* In the HA-LAESI source (Figure 1), the sample was introduced by mid-infrared (IR) laser ablation. The IR laser beam was produced by an optical parametric oscillator by converting the output of a Nd:YAG laser (Vibrant IR, Opotek, Carlsbad, CA) in the form of 5 ns pulses at 2.94 μm and a repetition rate of 5−10 Hz. The sample was placed on a glass microscope slide held in air or on a Peltier cooling stage 8−20 mm below the MS orifice (Figure 1d). The temperature of the cooled samples was measured using an adjustable focus remote infrared thermometer (845, Testo Inc., Sparta, NJ). The laser beam was guided with two gold-coated mirrors (PF10-03-M01, Thorlabs, Newton, MA) to pass vertically in front of the mass spectrometer inlet and focused with a 50-mm focal length planoconvex CaF_2 lens (Infrared Optical Products, Huntington, NY) to a small spot at the sample surface. The spot size was determined to be ∼300 μm in diameter by exposing thermal paper to the focused laser beam and measuring the dimensions of the burn marks under a microscope. The laser pulse energy at the target was 0.1 to 4 mJ/pulse, which corresponded to a fluence of 0.1 to 6 J/cm^2 for the given focusing conditions. Water has an absorption maximum at 2.94 μm[19] due to the OH bond vibrations. Therefore, the laser beam energy is rapidly deposited into the water molecules of the sample. This ultimately leads to phase explosion and the ablation of aqueous droplets or other water-rich samples, such as tissue. Here, the plume of particulates released from the sample surface was postionized with electrospray (ES). A nebulizer microchip was set to blow heated N_2 directly toward the mass spectrometer inlet, and an ES emitter was set to spray diagonally to the MS orifice, both in a horizontal plane with the MS inlet (Figure 1a). The heated nebulizer microchips have been previously described in detail.[20] The ES emitter was built in-house using a stainless steel t-connector, a conductive ferrule, and a needle port (all IDEX Health & Sciences, Oak Harbor, WA) to connect a 50 μm i.d. 320 μm o.d. stainless steel tapered-tip needle and a 100 μm i.d., 360 μm o.d. fused silica capillary (both New Objective Inc., Woburn, MA). The angle between the ES emitter and the microchip was ∼20−30°, the distance of the microchip nebulizer tip from the orifice was ∼8−10 mm, and the distance between the tip of the microchip spray nozzle and the tip of the ES emitter was ∼3−6 mm. The ES emitter was kept at high potential (2400−3600 V, 2800 V being optimal) by a dc high voltage power source PS350 from Stanford Research Systems Inc. (Sunnyvale, CA), and the ES solution was pumped through the emitter at 0.4 μL/min flow rate (a SP100I syringe pump, World Precision Instruments Inc., Sarasota, FL). The nitrogen flow rate was regulated between 0 and 480 mL/min and kept at 180 or 360 mL/min in the experiments as indicated later. The heating power of the chip was set between 0 and 4 W, and powers of 2.8−4.0 W (corresponding to temperatures of ∼170−220 °C at the nozzle) were used in the experiments as indicated below. The laser beam was set to pass between the spray axes of the ES emitter and the microchip, at ∼3 mm horizontal distance from the tip of the chip nozzle (y in Figure 1d).

LAESI. The LAESI setup (Figure 1b) was similar to that originally described by Nemes et al.[9] Briefly, the analytes were ablated by a mid-IR laser, as described above for HA-LAESI, and ionized using the ES emitter described above. The tip of the stainless steel needle emitter was set to point directly to the MS orifice at the same horizontal plane at ∼10 mm distance. High voltage was applied to the emitter (2800 V-3000 V) by the PS350 dc power source, and the ES solution was pumped through the needle at 0.4 μL/min using the SP100I syringe pump. The laser beam for the sample ablation was guided between the MS orifice and the ES needle, horizontally at ∼3−5 mm distance from the needle tip (y in Figure 1d).

LAAPPI. The LAAPPI source (Figure 1c) was almost identical to that described recently.[14] Briefly, the sample was ablated with a mid-IR laser as described above for HA-LAESI. The sample plume was intercepted with a heated toluene jet that was sprayed directly toward the orifice with the aid of nitrogen nebulizer gas using the heated nebulizer microchip and a Physio 22 syringe pump (Harvard Apparatus, Holliston,

dx.doi.org/10.1021/ac302432h | *Anal. Chem.* 2013, 85, 177−184

MA). The nebulizer gas (nitrogen) flow rate was controlled and measured using the GFC17 mass flow controller. Ionization of the toluene spray was induced with 10.0 and 10.6 eV photons emitted by a krypton discharge photoionization lamp (PKR 100 by Heraeus Noblelight, Cambridge, UK), after which the analytes were ionized via gas-phase reactions with the solvent ions.[14] The operational parameters were as follows: the sample was 8−20 mm below the axis of the orifice, the microchip nozzle was ∼10 mm from the orifice (x and y in Figure 1d were ∼8 and ∼2 mm, respectively), the spray solvent was toluene at 0.5 μL/min, the nebulizer gas was nitrogen at 80−100 mL/min, and the chip heating power was 2.9 W, which corresponds to a jet temperature of ∼300 °C.

RESULTS AND DISCUSSION

The novel HA-LAESI ion source (Figure 1a) was observed to enable the simultaneous detection of compounds of significantly varying polarities (completely nonpolar, weakly polar, polar, basic/acidic) as shown in Figure 2a for a mixture of

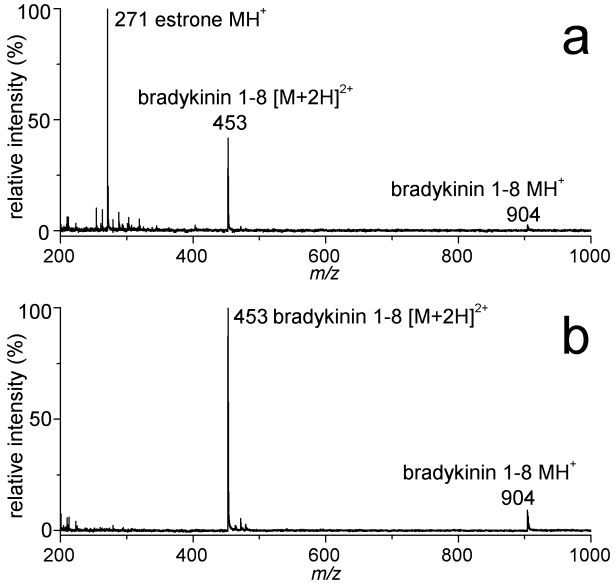

Figure 2. Analysis of a mixture of estrone (25 μM) and bradykinin 1−8 (23 μM) using the HA-LAESI ion source with (a) electrospray, N_2 gas flow (180 mL/min), and heating turned on (2.8 W), and (b) electrospray on but N_2 gas flow and heating turned off (LAESI mode). The background has been subtracted from both spectra.

bradykinin 1−8 and estrone solutions (See Figure S1 in Supporting Information for the structures and Table S1 for the polar surface areas, and pK_a and log P values of the analytes used in this study). It was confirmed that the ablated sample was ionized by the electrospray, because when the source was operated with the ES emitter voltage turned off, no analyte or background signal was observed. The hot stream of nitrogen was found to be essential for the ionization of estrone, which showed no signal without the gas flow (Figure 2b), whereas the bradykinin 1−8 appeared as MH^+ and $[M + 2H]^{2+}$ ions in the LAESI mode, as well. Conventional LAESI typically shows high ionization efficiency for peptides, but its ionization efficiency for nonpolar steroids is low.

Effect of the Gas Temperature and Flow Rate. The effect of the gas temperature was studied by varying the microchip heating power between 0 and 4.0 W, corresponding to jet temperatures between ambient and above 200 °C. Estrone did not produce a signal at heating powers below 2.0 W, corresponding to jet temperatures of approximately 100−150 °C. Above 2.0 W, the signal of estrone increased as the microchip heating power was increased up to 3.0 W, as shown in Figure 3a, whereas the signal of bradykinin 1−8 was

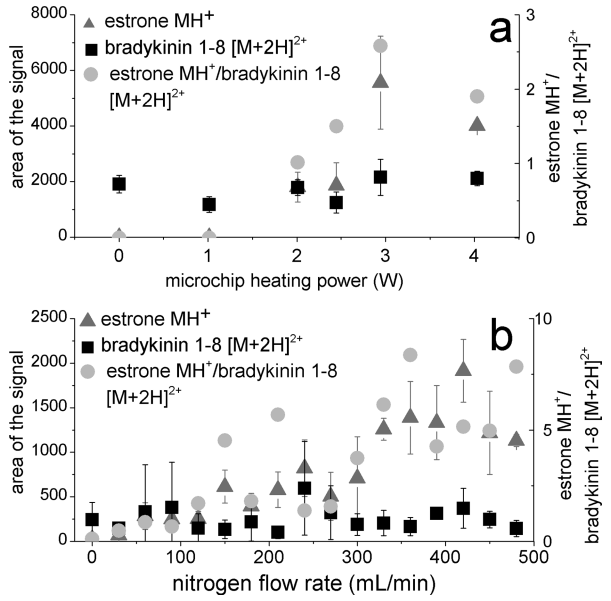

Figure 3. The integrated areas of signals of estrone MH^+ and bradykinin $[M + 2H]^{2+}$ ions and the ratio of the areas at (a) different heating powers and a constant N_2 flow rate of 360 mL/min and ES voltage 2800 V, and at (b) different N_2 flow rates and a constant heating power of 2.5 W and ES voltage 3600 V. The given values are three-sample averages, and the error bars show the standard deviations.

somewhat independent of the gas temperature. Figure 3b shows the signals for estrone MH^+ and bradykinin 1−8 $[M + 2H]^{2+}$ ions and the ratio of the signals at different gas flow rates at a constant heating power of the microchip. ES voltages at the measurements were different, and therefore the signal of bradykinin 1−8 is lower in b, likely because of fragmentation. Again, the signal of estrone grew with the increasing flow rate up to 330 mL/min, whereas the signal of bradykinin 1−8 was somewhat independent of the used flow rate.

Heated gas flow has been reported to enhance the ionization efficiency in ESI due to increased evaporation rate[21] and reduced surface tension of the ES droplets,[22] and this phenomenon has been utilized in commercial ion spray sources, such as, for example, the TurboIonSpray[21] and the Jet Stream. However, the solution flow rates applied in ion spray are typically much higher (5−1000 μL/min); thus, the initial droplets are expected to be significantly larger than in HA-LAESI, which uses very low flow rates (0.4 μL/min). Also, the use of the heated gas flow in ion spray enhances the signal of both nonpolar[23] and polar compounds.[24−26] Thus, more efficient evaporation of the solvent from the ES droplets is probably not the sole reason for the enhanced ionization efficiency of estrone in HA-LAESI.

In HA-LAESI, changes in droplet size may affect the fusion of the sample projectiles and the ES droplets. The hot gas jet may also cause the evaporation of the ablated sample droplets, and vaporization of the analytes could lead to the secondary electrospray ionization (SESI)[27] type of ionization of the

dx.doi.org/10.1021/ac302432h | Anal. Chem. 2013, 85, 177−184

Table 1. Ions Observed for the Selected Analytes by HA-LAESI[a]

analyte	observed ions (m/z, relative peak height in parentheses)	
	MH^+	other observed ions
bradykinin 1−8	904.4 (14)	452.7 ($[M + 2H]^{2+}$, 100)
cholecalciferol	385.3 (100)	–
cholesterol	–	369.3 ($[MH - H_2O]^+$, 100)
DHEA	289.2 (100)	271.2 ($[MH - H_2O]^+$, 10), 306.2 ($[M + NH_4]^+$, 11), 311.2 ($[M + Na]^+$, 5), 321.2 ($[MH+CH_3OH]^+$ or $[MH+O_2]^+$, 14), 577.4 ($[2M + H]^+$, 7)
DOPC	786.6 (100)	808.5 ($[M + Na]^+$, 17)
estrone	271.2 (100)	–
fucose	–	129.1 ($[MH - 2H_2O]^+$, 32), 147.1 ($[MH - H_2O]^+$, 48), 164.1 ($[M-H_2O+NH_4]^+$, 72), 182.1 ($[M + NH_4]^+$, 100), 187.1 ($[M + Na]^+$, 24), 351.1 ($[2M + Na]^+$, 20)
lysozyme	–	1193 ($[M + 12H]^{12+}$, 32), 1301 ($[M + 11H]^{11+}$, 74), 1432 ($[M + 10H]^{10+}$, 100), 1590 ($[M + 9H]^{9+}$, 85), 1789 ($[M + 8H]^{8+}$, 30)
naphtho[2,3-*a*] pyrene	303.1 (100)	–
DG(34:1)	595.5 (15)	265.2 (6), 313.3 ($[MH - FA(18:1)]^+$, 37), 339.3 [$MH - FA(16:0)]^+$, 29), 577.5 ($[MH - H_2O]^+$, 100), 612.6 ($[M + NH_4]^+$, 15), 617.5 ($[M + Na]^+$, 11)
perylene	253.1 (100)	–
TMCL	–	495.4 (37), 513.4 (100), 530.5 (29), 535.4 (12)
tricaprylin	471.3 (96)	327.2 ($[MH - FA(8:0)]^+$, 100), 345.2 (14), 488.4 ($[M + NH_4]^+$, 34), 493.3 ($[M + Na]^+$, 29)
verapamil	455.3 (100)	–

[a]Ions with relative intensity of 5% or higher are reported. The compounds were analyzed from their 100 μM solution in methanol/water (1:1, v:v), except for estrone (25 μM) and bradykinin (23 μM) that were analyzed from their mixture and for lysozyme that was used as a 350 μM solution prepared in water. The N_2 flow rate was 360 mL/min, and the microchip heating power was 2.8 W. FA = fatty acid.

analytes by gas-phase reactions[28,29] with the ES generated ions. SESI is expected to have better ionization efficiency for low polarity analytes than ESI, because although the liquid-phase basicities of these compounds are too low to lead to ionization in the liquid phase as required in ESI, their gas-phase proton affinities can be sufficiently high to be ionized in the gas phase. The heated gas flow may also reduce the cluster size of charged ES and sample solvent species, and because the proton affinities of smaller water and methanol clusters are lower than those of large clusters,[30−32] this may improve the gas-phase ionization efficiency of compounds with low proton affinity. The more detailed studies needed to establish the mechanisms involved are beyond the scope of this report.

Analyte Ions. The HA-LAESI method was tested for the analysis of a variety of compounds listed in Table 1. MH^+ ions were detected for most of the studied analytes. In addition to verapamil, bradykinin 1−8, and lysozyme that are charged in solution, also compounds that have few or no polarizable atoms and no proton-accepting basic groups (Table S1 in Supporting Information) were found to protonate readily in HA-LAESI. Even the completely nonpolar polyaromatic hydrocarbons (PAH) perylene and naphtho[2,3-*a*]pyrene showed MH^+ ions. Ammonium and sodium adducts were observed for DHEA, fucose, tricaprylin, and DG(34:1). Cholesterol was observed at m/z 369.3 corresponding to $[MH - H_2O]^+$, and similar fragment ions were also observed for DG(34:1) and fucose. Tricaprylin and DG(34:1) showed fragments due to the loss of fatty acid chains, and TMCL showed fragments that were not identified.

Figure 4 shows the analysis of a mixture of tricaprylin, TMCL, cholesterol, bradykinin 1−8, and DG(34:1) using HA-LAESI, conventional LAESI, and LAAPPI, and Figure S2 in Supporting Information shows the analysis of a mixture of cholecalciferol, pyrene, fucose, DOPC, and lysozyme with the same techniques. TMCL, cholesterol, and DG(34:1) were efficiently ionized using HA-LAESI and LAAPPI but not with conventional LAESI. Cholesterol has been detected from mouse and rat brain by conventional LAESI as the $[MH - H_2O]^+$ ion in previous studies,[33,34] but its concentration in the brain is expected to be much higher than used here (100 μM). Conventional LAESI showed only minor peaks for tricaprylin and cholecalciferol as MH^+, and tricaprylin as $[M + NH_4]^+$ and $[M + Na]^+$ ions, whereas with HA-LAESI these analytes showed the most abundant signals. Cholecalciferol, cholesterol, DG(34:1), and tricaprylin are neutral lipids, which are typically derivatized before ESI analysis or analyzed utilizing adduct formation (with, for example, NH_4^+ ions).[35] The ionization of bradykinin 1−8, fucose, and lysozyme was achieved using both conventional and HA-LAESI. The multiply charged and adduct ion species ($[M + nH]^{n+}$, $[M + NH_4]^+$, and $[M + Na]^+$) observed for the studied compounds in HA-LAESI resembled those typically observed in ESI and LAESI and were likely to have formed in an ionization process involving the charged droplets. However, the less polar compounds, which were not ionized in LAESI but only in HA-LAESI, could have also been ionized through gas-phase ion/molecule reactions. LAAPPI did not ionize bradykinin 1−8, fucose, and lysozyme, which may partly be due to fragmentation caused by the applied hot solvent jet (80−100 mL/min). Because of the microchip heat transfer properties and higher gas flow rate applied in HA-LAESI (360 mL/min), the temperature of the jet is lower in HA-LAESI than in LAAPPI.[36] Additionally, the ES droplets may absorb some of the energy in HA-LAESI. Pyrene could only be ionized with LAAPPI, where it formed a radical cation ($M^{+\bullet}$). Also cholesterol, tricaprylin, cholecalciferol, and DG(34:1) were ionized in LAAPPI, because LAAPPI utilizes photon induced gas-phase reactions that can ionize the studied analytes similarly as reported for lipids in atmospheric pressure photoionization[37,38] and DAPPI.[39]

Quantitative Performance. Limits of detection (LODs) were measured for estrone, bradykinin 1−8, and verapamil by analyzing 0.5 μL samples by HA-LAESI. The samples were kept at −4 °C to 7 °C on a cooled Peltier stage to avoid drying, which would prevent the ablation of the sample. While freezing

dx.doi.org/10.1021/ac302432h | *Anal. Chem.* 2013, 85, 177−184

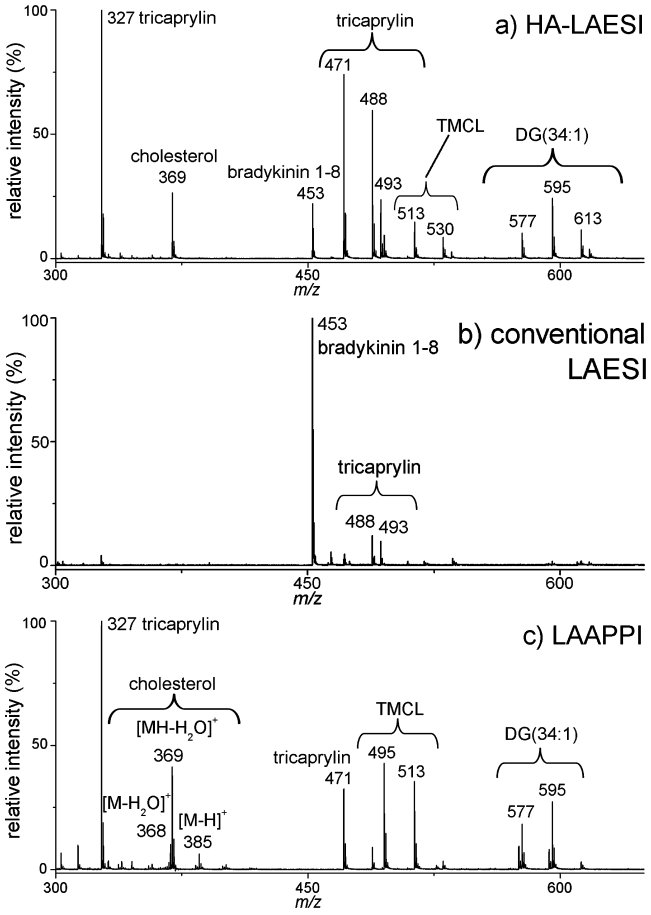

Figure 4. Analysis of 10 μL of a mixture of cholesterol (100 μM), tricaprylin (100 μM), bradykinin 1−8 (92 μM), 1-palmitoyl-2-oleoyl-*sn*-glycerol (DG(34:1), 100 μM), and 1,1′,2,2′-tetramyristoyl cardiolipin (TMCL, 100 μM) using HA-LAESI, conventional LAESI, and LAAPPI. See Table 1 for assignment of the ions. In HA-LAESI the N_2 gas flow rate was 360 mL/min and the microchip heating power was 2.8 W. Background has been subtracted from all three spectra.

can result in dramatic changes in the IR laser ablation of a target, it was not an issue here, as the samples were prepared in methanol/water (1:1) mixture with a freezing point well below the temperature of the samples. The time-resolved intensities of analyte ions (MH^+ for estrone and verapamil, $[M + 2H]^{2+}$ for bradykinin 1−8) were monitored and the absolute amounts giving a signal-to-noise ratio ≥3 were 3, 1.2, and 0.13 pmol for estrone, bradykinin 1−8, and verapamil, respectively. The LOD for bradykinin 1−8 by conventional LAESI was 0.6 pmol, slightly better than that obtained with HA-LAESI. The lower sensitivity for bradykinin 1−8 in HA-LAESI is likely due to the elevated temperature of the ion source that could induce the fragmentation of the peptide, or to the different ion source geometry. We also determined the LOD for estrone using LAAPPI, where it was detected as the $M^{+\cdot}$ ion, and a similar LOD (3 pmol) was obtained as with HA-LAESI. Previous studies on conventional LAESI[9] and LAAPPI[14] have reported similar sensitivities for verapamil (236[9] and 250 nM, respectively) as observed here by HA-LAESI (250 nM). Comparison of HA-LAESI with DEMI,[15] another ambient ionization technique with a broad range of ionization capability, shows that the absolute LODs obtained with HA-LAESI are ∼2 orders of magnitude better than those reported previously for angiotensin I and dibromodibenzosuberone by DEMI. The comparison of HA-LAESI LODs with those achieved with DESI (e.g., 0.7 pg for bradykinin and 0.1−2000 pg (≈0.04−7000 fmol) for other selected analytes)[40] and DAPPI (0.056 pmol for verapamil and 0.083 pmol for testosterone)[13] shows that for these particular compounds, HA-LAESI is slightly less sensitive than DESI and DAPPI, although this may be partly due to the old mass spectrometer used in our work and the full scan MS data application mode used.

As controlling the repeatability of the sampling was difficult for the 0.5 μL droplets, the linearity of HA-LAESI was tested by analyzing 10 μL droplets of verapamil at concentration levels ranging from 500 nM to 1.0 mM, corresponding to 5.0 pmol to 10 nmol in absolute amounts. The quantitation was performed based on the area of the signal that was obtained by the ablation of the whole sample volume to compensate for any differences in experimental conditions throughout the measurement, such as changes in the evaporation rate of the droplets or inconsistency in the manual pipetting of the droplet to the sample holder. The signal was found to be linear over the three studied decades (n = 11) with R^2 = 0.988 as shown in Figure S3 in Supporting Information. The relative standard deviation (RSD) for the signal of 3 droplets of 100 μM solution was 21%, and the average RSD over the whole studied concentrations range (n = 11) was 22% (n = 3). This indicates semiquantitative performance typical of ambient MS techniques without the use of an internal standard.

Applications. Solid biological tissues that contain endogenous water were studied by HA-LAESI, as it is known that they can be sampled by IR laser ablation at 2.94 μm.[41]

Avocado Mesocarp. Figure 5 shows the analysis of lipids from a 0.5 mm section of avocado (*Persea Americana*) mesocarp using conventional and HA-LAESI. The spectra obtained by the two techniques were observed to be distinctly different. HA-LAESI showed abundant ions at m/z 550−640 and 800−910. The m/z values of the majority of the abundant ions correspond to those of the triglyceride (TG) ions listed in

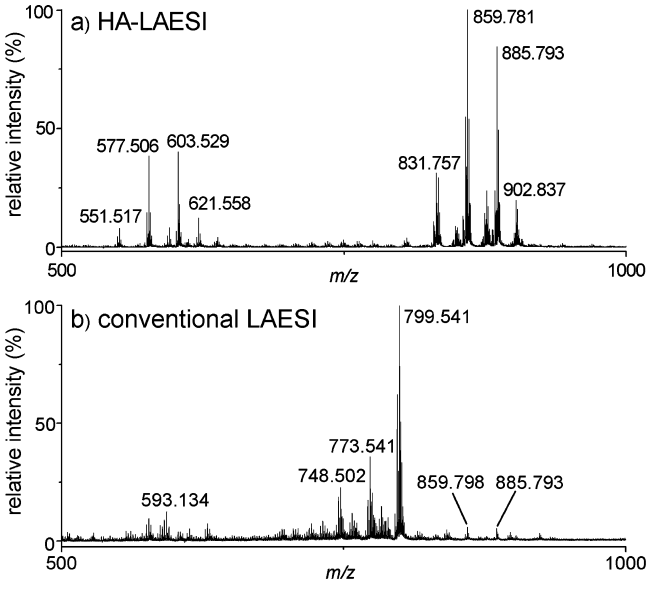

Figure 5. Typical mass spectrum of a 0.5 mm thick avocado tissue section obtained using (a) HA-LAESI and (b) conventional LAESI. In HA-LAESI the N_2 flow rate was 360 mL/min and the microchip heating power was 4.0 W. The sample was kept at ∼2 °C by a cooled Peltier stage during the experiment.

dx.doi.org/10.1021/ac302432h | *Anal. Chem.* 2013, 85, 177−184

Table S2 in the Supporting Information, and they are consistent with the previously determined TG composition of avocado oil.[42,43] Conventional LAESI showed only minor peaks for the ions with the m/z values corresponding to TG ions (Figure 5b). Previous studies on avocado showed the pulp to contain plenty of lipids (~10−20% of the pulp),[44,45] and over 95% of the lipids were TGs.[44] This clearly indicates that HA-LAESI has significantly better ionization efficiency for nonpolar compounds compared to conventional LAESI. The lipid region of the conventional LAESI spectrum was rich with ions that were thought to be due to more polar lipids, possibly phospholipids and monogalactosyl diglycerides (Table S3 in Supporting Information), which were most likely suppressed by the more abundant TGs in HA-LAESI.

Mouse Brain Tissue. Figure 6 shows a spectrum of a 40 μm thick mouse brain tissue section analyzed by HA-LAESI.

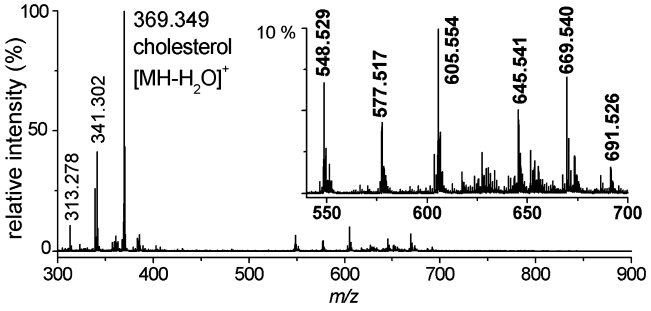

Figure 6. A typical HA-LAESI spectrum of a 40 μm thick mouse brain tissue. The N_2 flow rate was 360 mL/min, and the microchip heating power was 4.0 W. The sample was kept at ~2 °C by a cooled Peltier stage during the experiment.

The base peak in the brain tissue spectra was at m/z 369.349, corresponding to the cholesterol $[MH - H_2O]^+$ ion. In previous studies of mouse and rat brain tissues by conventional LAESI, cholesterol was observed with much lower sensitivity than here.[33,34] Cholesterol is one of the most abundant lipids in brain tissue, and HA-LAESI provided better ionization efficiency for the nonpolar lipid compared to conventional LAESI. In fact, the results obtained by HA-LAESI resemble those obtained by LAAPPI in a previous work,[14] which showed abundant $[M - H_2O]^{+\cdot}$, $[MH - H_2O]^+$, $[M - H]^+$ and $M^{+\cdot}$ ions for cholesterol. Preliminary assignments for other ions observed by HA-LAESI are listed in Table S4 in Supporting Information. In addition, some areas of the brain section showed minor signals at m/z 700−800 corresponding to phospholipid ions. Accurate mass determinations and MS/MS analyses would be required to reliably identify all the observed ions, but the presented results for avocado and mouse brain tissue clearly show that HA-LAESI ionizes low polarity constituents more efficiently than conventional LAESI.

Pansy Petals. The heat-assisted LAESI was compared with conventional LAESI also in the analysis of pansy (*Viola*) petals. The two techniques gave similar spectra for the petals as shown in Figure S4 in Supporting Information. The major ions were detected at m/z 611.2 (yellow tissue), 903.3 (purple tissue), and 919.3 (purple tissue) and were thought to correspond to previously established flavonol and anthocyanidin glycosides of *Viola*, namely rutin[46] MH^+, cyanidin-3-*p*-coumaroylrhamnosyl-glucoside-5-glucoside[47] M^+, and delphinidin-3-*p*-coumaroylr-hamnosylglucoside-5-glucoside[47,48] M^+, respectively. The spatial distribution of the ion at m/z 919.3 is shown in Figure 7. This demonstrates that HA-LAESI can also be applied to mass spectrometry imaging.

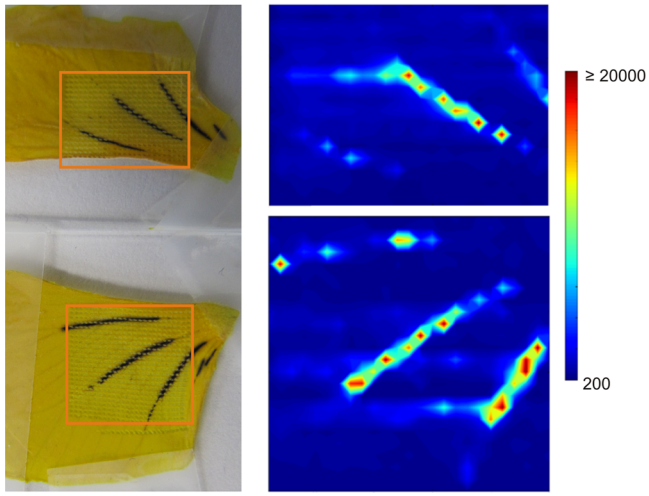

Figure 7. A photograph of the studied pansy petal and the spatial distribution of the ion at m/z 919.3 measured using conventional LAESI (top, plot size 9.6 × 6.8 mm) and HA-LAESI (bottom, plot size 9.6 × 9.2 mm). The orange squares on the photo show the approximate studied areas corresponding to the 2D contour plots. The sample was kept at ~2 °C by a cooled Peltier stage during the experiment to avoid dehydration of the tissue. The sampling step size was 0.4 mm and dwell time 8 s.

CONCLUSIONS

Efficient ionization of nonpolar and polar analytes of diverse sizes was achieved in LAESI by intercepting the electrospray and sample plumes with a heated gas jet. The improved ionization efficiency for low polarity analytes was thought to be due to enhanced evaporation of solvent from the electrospray and the sample droplets, and a mechanism resembling secondary electrospray ionization that allows ionization of low polarity compounds in the gas phase. However, more detailed studies beyond the scope of this report are needed to establish the mechanism. HA-LAESI was shown to be feasible for the analysis of neutral and polar lipids directly from solid plant and animal tissues containing endogenous water, where it ionized compounds of a wider polarity range than that for conventional LAESI. We expect the technique to be applicable also to solid samples containing water ice or other chemicals that can be excited by IR irradiation. Because the narrow beam of the IR laser used in HA-LAESI has been found to provide sufficient spatial resolution for imaging applications, we expect HA-LAESI to become an efficient tool for the imaging of both polar and nonpolar compounds of various sizes.

ASSOCIATED CONTENT

Supporting Information

Additional information as noted in the text. This material is available free of charge via the Internet at http://pubs.acs.org.

AUTHOR INFORMATION

Corresponding Author

*A.V.: Tel. +1 (202) 994-2717. Fax. +1 (202) 994-5873. E-mail: vertes@gwu.edu. T.J.K.: Tel. +358 9 191 59169. Fax. +358 9 191 59556. E-mail: tiina.kauppila@helsinki.fi.

Notes

The authors declare no competing financial interest.

■ ACKNOWLEDGMENTS

A. Vaikkinen, T.J.K., and R.K. acknowledge the Academy of Finland (project numbers 218150, 125758, 255559, and 251575) and CHEMSEM graduate school for funding the study. A. Vertes and B.S. acknowledge financial support from the U.S. Department of Energy (Grant DEFG02-01ER15129), Protea Biosciences Group, Inc., and the George Washington University Selective Excellence Fund.

■ REFERENCES

(1) Van Berkel, G. J.; Pasilis, S. P.; Ovchinnikova, O. *J. Mass Spectrom.* **2008**, *43*, 1161−1180.
(2) Alberici, R. M.; Simas, R. C.; Sanvido, G. B.; Romão, W.; Lalli, P. M.; Benassi, M.; Cunha, I. B. S.; Eberlin, M. N. *Anal. Bioanal. Chem.* **2010**, *398*, 265−294.
(3) Amstalden van Hove, E. R.; Smith, D. F.; Heeren, R. M. A. *J. Chromatogr., A* **2010**, *1217*, 3946−3954.
(4) Shrestha, B.; Vertes, A. *Anal. Chem.* **2009**, *81*, 8265−8271.
(5) Tanaka, K.; Waki, H.; Ido, Y.; Akita, S.; Yoshida, Y.; Yohida, T. *Rapid Commun. Mass Spectrom.* **1988**, *2*, 151−153.
(6) Spengler, B.; Hubert, M. *J. Am. Soc. Mass Spectrom.* **2002**, *13*, 735−748.
(7) Guerquin-Kern, J.; Wu, T.; Quintana, C.; Croisy, A. *Biochim. Biophys. Acta* **2005**, *1724*, 228−238.
(8) Takáts, Z.; Wiseman, J. M.; Gologan, B.; Cooks, R. G. *Science* **2004**, *306*, 471−473.
(9) Nemes, P.; Vertes, A. *Anal. Chem.* **2007**, *79*, 8098−8106.
(10) Shiea, J.; Huang, M.-Z.; Hsu, H.-J.; Lee, C.-Y.; Yuan, C.-H.; Beech, I.; Sunner, J. *Rapid Commun. Mass Spectrom.* **2005**, *19*, 3701−3704.
(11) Sampson, J. S.; Hawkridge, A. M.; Muddiman, D. C. *J. Am. Soc. Mass Spectrom.* **2006**, *17*, 1712−1716.
(12) Cody, R. B.; Laramee, J. A.; Durst, H. D. *Anal. Chem.* **2005**, *77*, 2297−2302.
(13) Haapala, M.; Pól, J.; Saarela, V.; Arvola, V.; Kotiaho, T.; Ketola, R. A.; Franssila, S.; Kauppila, T. J.; Kostiainen, R. *Anal. Chem.* **2007**, *79*, 7867−7872.
(14) Vaikkinen, A.; Shrestha, B.; Kauppila, T. J.; Vertes, A.; Kostiainen, R. *Anal. Chem.* **2012**, *84*, 1630−1636.
(15) Nyadong, L.; Galhena, A. S.; Fernández, F. M. *Anal. Chem.* **2009**, *81*, 7788−7794.
(16) Chan, C.; Bolgar, M. S.; Miller, S. A.; Attygalle, A. B. *J. Am. Soc. Mass Spectrom.* **2011**, *22*, 173−178.
(17) Shrestha, B.; Patt, J. M.; Vertes, A. *Anal. Chem.* **2011**, *83*, 2947−2955.
(18) Nemes, P.; Barton, A. A.; Li, Y.; Vertes, A. *Anal. Chem.* **2008**, *80*, 4575−4582.
(19) Shori, R. K.; Walston, A. A.; Stafsudd, O. M.; Fried, D.; Walsh, J. T., Jr. *IEEE J. Sel. Top. Quantum Electron.* **2001**, *7*, 959−970.
(20) Saarela, V.; Haapala, M.; Kostiainen, R.; Kotiaho, T.; Franssila, S. *Lab Chip* **2007**, *7*, 644−646.
(21) Li, L.; Campbell, D.; Bennett, P.; Henion, J. *Anal. Chem.* **1996**, *68*, 3397−3404.
(22) Lu, W.; Bennett, B. D.; Rabinowitz, J. D. *J. Chromatogr., B* **2008**, *871*, 236−242.
(23) Careri, M.; Elviri, L.; Mangia, A. *J. Chromatogr., A* **1999**, *854*, 233−244.
(24) Boscaro, F.; Pieraccini, G.; La Marca, G.; Bartolucci, G.; Luceri, C.; Luceri, F.; Moneti, G. *Rapid Commun. Mass Spectrom.* **2002**, *16*, 1507−1514.
(25) Hu, C.-W.; Chao, M.-R.; Sie, C.-H. *Free Radic. Biol. Med.* **2010**, *48*, 89−97.
(26) Ferrer, I.; Thurman, E. M.; Zweigenbaum, J. A. Ultrasensitive EPA Method 1694 with the Agilent 6460 ESI/MS/MS with Jet Stream Technology for Pharmaceuticals and Personal Care Products in Water, Application Note, 2010, Agilent Technologies. http://www.chem.agilent.com/library/applications/5990-4605en.pdf (accessed 7/18/2012).
(27) Fernandez De La Mora, J. *Int. J. Mass Spectrom.* **2011**, *300*, 182−193.
(28) Martinez-Lozano Sinues, P.; Criado, E.; Vidal, G. *Int. J. Mass Spectrom.* **2012**, *313*, 21−29.
(29) Tam, M.; Hill, H. H., Jr. *Anal. Chem.* **2004**, *76*, 2741−2747.
(30) Knochenmuss, R.; Cheshnovsky, O.; Leutwyler, S. *Chem. Phys. Lett.* **1988**, *144*, 317−323.
(31) Meot-Ner, M. *J. Am. Chem. Soc.* **1986**, *108*, 6189−6197.
(32) Grimsrud, E. P.; Kebarle, P. *J. Am. Chem. Soc.* **1973**, *95*, 7939−7943.
(33) Nemes, P.; Woods, A. S.; Vertes, A. *Anal. Chem.* **2010**, *82*, 982−988.
(34) Shrestha, B.; Nemes, P.; Nazarian, J.; Hathout, Y.; Hoffman, E. P.; Vertes, A. *Analyst* **2010**, *135*, 751−758.
(35) Murphy, R. C.; Fiedler, J.; Hevko, J. *Chem. Rev.* **2001**, *101*, 479−526.
(36) Saarela, V.; Haapala, M.; Kostiainen, R.; Kotiaho, T.; Franssila, S. *J. Micromech. Microeng.* **2009**, *19*, 055001.
(37) Gaudin, M.; Imbert, L.; Libong, D.; Chaminade, P.; Brunelle, A.; Touboul, D.; Laprevote, O. *J. Am. Soc. Mass Spectrom.* **2012**, *23*, 869−879.
(38) Cai, S.-S.; Syage, J. A. *Anal. Chem.* **2006**, *78*, 1191−1199.
(39) Suni, N. M.; Aalto, H.; Kauppila, T. J.; Kotiaho, T.; Kostiainen, R. *J. Mass. Spectrom.* **2012**, *47*, 611−619.
(40) Takáts, Z.; Wiseman, J.; Cooks, R. *J. Mass Spectrom.* **2005**, *40*, 1261−1275.
(41) Vogel, A.; Venugopalan, V. *Chem. Rev.* **2003**, *103*, 577−644.
(42) Lísa, M.; Holčapek, M. *J. Chromatogr., A* **2008**, *1198−1199*, 115−130.
(43) Jakab, A.; Héberger, K.; Forgács, E. *J. Chromatogr., A* **2002**, *976*, 255−263.
(44) Takenaga, F.; Matsuyama, K.; Abe, S.; Torii, Y.; Itoh, S. *J. Oleo Sci.* **2008**, *57*, 591−597.
(45) Pacetti, D.; Boselli, E.; Lucci, P.; Frega, N. G. *J. Chromatogr. A* **2007**, *1150*, 241−251.
(46) Vukics, V.; Kery, A.; Guttman, A. *J. Chromatogr. Sci.* **2008**, *46*, 823−827.
(47) Zhang, J.; Wang, L.-S.; Gao, J.-M.; Xu, Y.-J.; Li, L.-F.; Li, C.-H. *Phytochem. Anal.* **2012**, *23*, 16−22.
(48) Saito, N.; Timberlake, C. F.; Tucknott, O. G.; Lewis, I. A. S. *Phytochemistry* **1983**, *22*, 1007−1009.

Supporting Information for

Simultaneous Detection of Nonpolar and Polar Compounds by Heat-Assisted Laser Ablation Electrospray Ionization-Mass Spectrometry

Anu Vaikkinen,[a, b] Bindesh Shrestha,[b] Javad Nazarian,[c] Risto Kostiainen,[a] Akos Vertes[b] and Tiina J. Kauppila[a]**

[a] Division of Pharmaceutical Chemistry, Faculty of Pharmacy, P.O. Box 56, 00014, University of Helsinki, Finland

[b] Department of Chemistry, W. M. Keck Institute for Proteomics Technology and Applications, George Washington University, Washington, DC 20052, USA

[c] Research Center for Genetic Medicine, Children's National Medical Center, Washington, DC 20010, USA, Department of Integrative Systems Biology, School of Medicine and Health Sciences, George Washington University, Washington, DC 20037, USA

Table S1: Details of the stock solutions, and the polar surface areas, pK_a and logP values of the analytes. * commercial solution ** Taken from SciFinder (scifinder.cas.org, accessed 5.11.2012): values are calculated using Advanced Chemistry Development (ACD/Labs) Software V11.02 (© 1994-2012 ACD/Labs). N.A. = not available.

Analyte	Polar Surface Area (A^2)**	**pK_a****	**log P****	**Stock solution**	
				c	**solvent**
bradykinin 1-8	323	3.56±0.10; 13.71±0.70	-3.280±0.935	5 mg/mL	water
cholecalciferol	20.2	14.74±0.20	9.085±0.342	10 mM	methanol
cholesterol	20.2	15.03±0.70	9.619±0.281	10 mM	methanol
dehydroepiandrosterone (DHEA)	37.3	15.02±0.60	3.305±0.342	10 mM	methanol
1,2-dioleoyl-*sn*-glycero-3-phosphocholine (DOPC)	N.A.	N.A.	N.A.	1 mg/mL	methanol
estrone	37.3	10.25±0.40	3.624±0.369	1 mM	methanol
fucose	98.0	12.50±0.20	-2.459±0.714	10 mM	water
lysozyme	N.A.	N.A.	N.A.	5 mg/mL	water
naphtho[2,3-*a*]pyrene	0.00	N.A.	7.372±0.182	1 mM	toluene
1-palmitoyl-2-oleoyl-***sn***-glycerol DG(34:1)*	72.8	13.69±0.10	14.427±0.443	2 mg/mL	chloroform
perylene	0.00	N.A.	6.188±0.178	10 mM	toluene
pyrene	0.00	N.A.	5.004±0.174	10 mM	toluene
1,1',2,2'-tetramyristoyl cardiolipin (TMCL)	257	1.07±0.50	22.740±0.551	1 mg/mL	methanol
tricaprylin	78.9	N.A.	9.387±0.264	10 mM	methanol
verapamil	64.0	8.97±0.50	4.024±0.380	10 mM	methanol

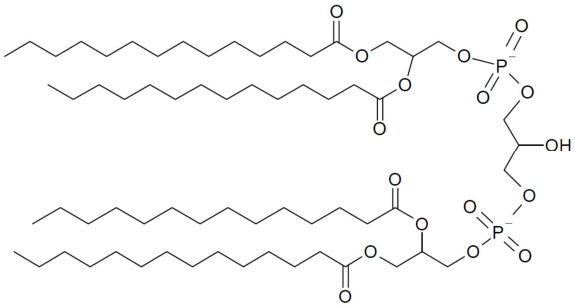

1,1',2,2'-tetramyristoyl cardiolipin (TMCL)
Monoisotopic mass = 1238.83 Da

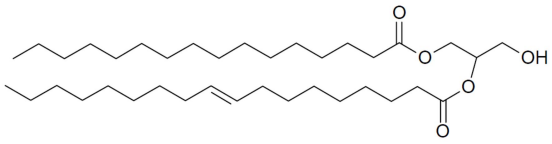

1-palmitoyl-2-oleoyl-*sn*-glycerol (DG(34:1))
Monoisotopic mass = 594.522 Da

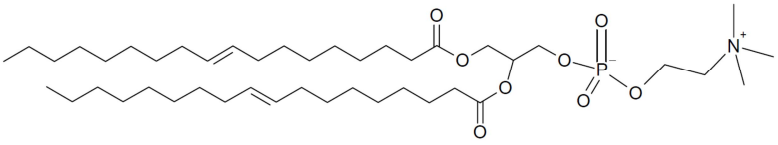

1,2-dioleoyl-*sn*-glycero-3-phosphocholine (DOPC)
Monoisotopic mass = 785.593 Da

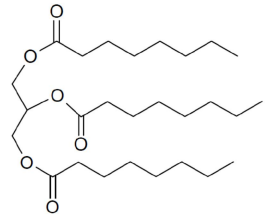

glyceryl trioctanoate (tricaprylin)
Monoisotopic mass = 470.361 Da

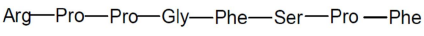

bradykinin fragment 1-8
Monoisotopic mass = 903.460 Da

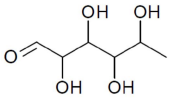

fucose
Monoisotopic mass = 164.068 Da

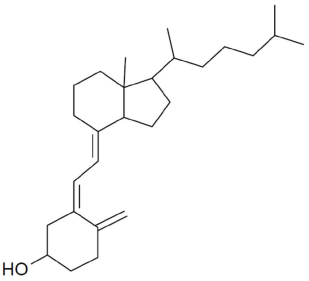

cholecalciferol
Monoisotopic mass = 384.339 Da

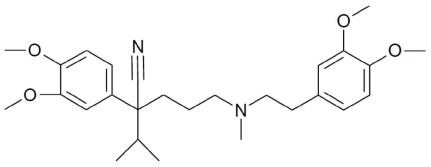

verapamil
Monoisotopic mass = 454.283 Da

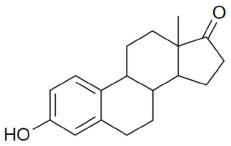

estrone
Monoisotopic mass = 270.162 Da

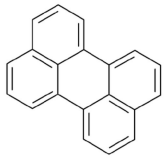

perylene
Monoisotopic mass = 252.094 Da

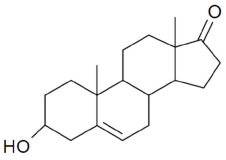

dehydroepiandrosterone (DHEA)
Monoisotopic mass = 288.209 Da

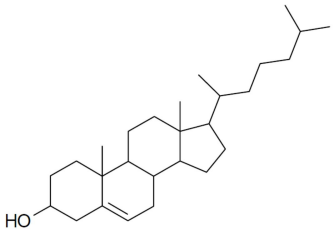

cholesterol
Monoisotopic mass = 386.355 Da

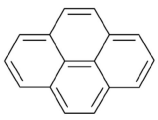

pyrene
Monoisotopic mass = 202.078 Da

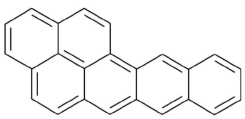

naphtho[2,3-*a*]pyrene
Monoisotopic mass = 302.110 Da

Figure S1: Structures of the analytes used in this study.

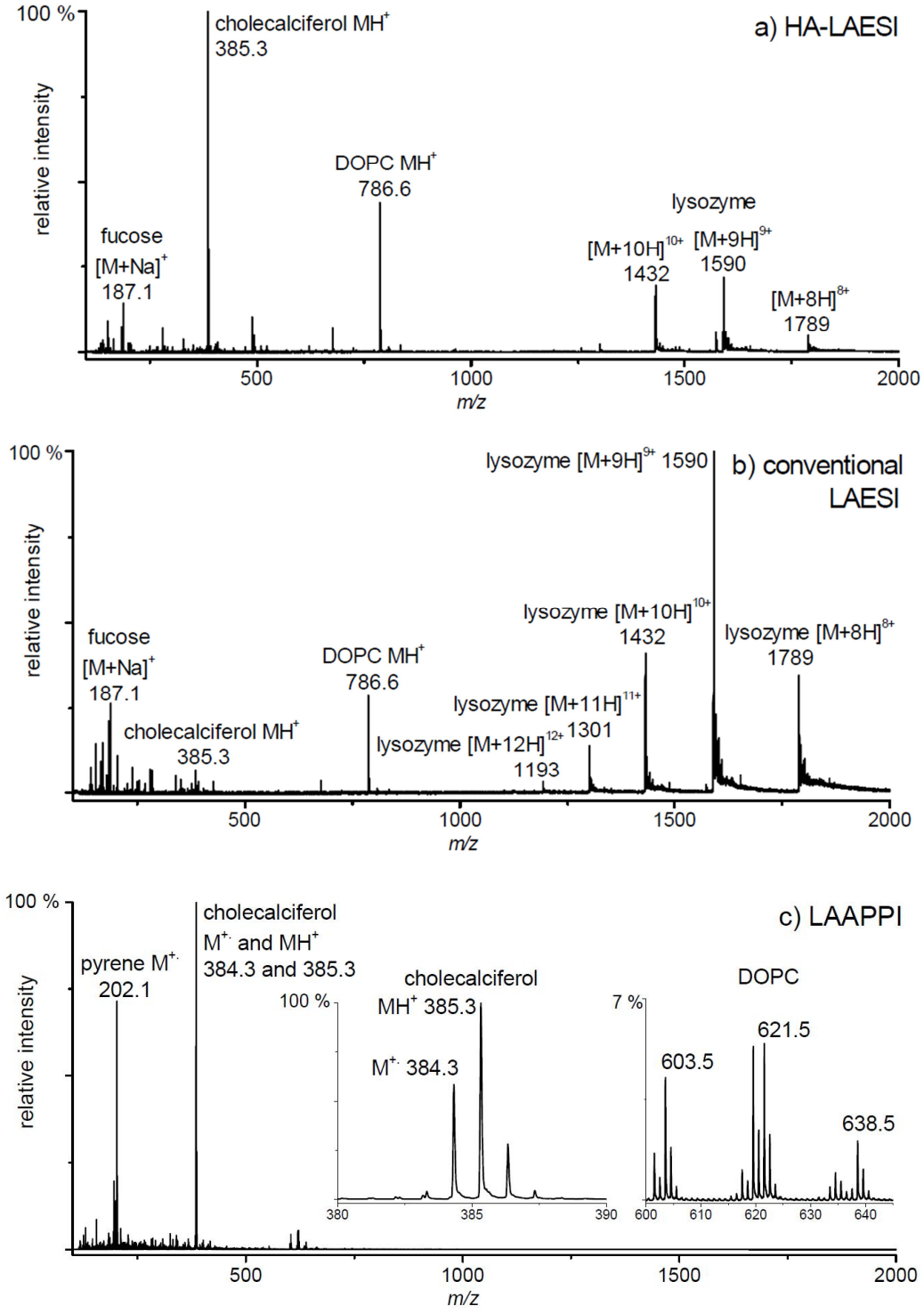

Figure S2: Analysis of mixture of cholecalciferol (100 µM), pyrene (100 µM), fucose (100 µM), DOPC (1,2-dioleoyl-sn-glycero-3-phosphocholine, 100 µM) and lysozyme (35 µM) using a) HA-LAESI, b) conventional LAESI, and c) LAAPPI. In LAAPPI the ions of DOPC are most likely due to the loss of the polar head group (*m/z* 603.5, 619.5, 621.5, and 638.5). Note that pyrene and cholecalciferol form radical cations ($M^{+\cdot}$) in LAAPPI, whereas $M^{+\cdot}$ ions were not observed in HA-LAESI or conventional LAESI.

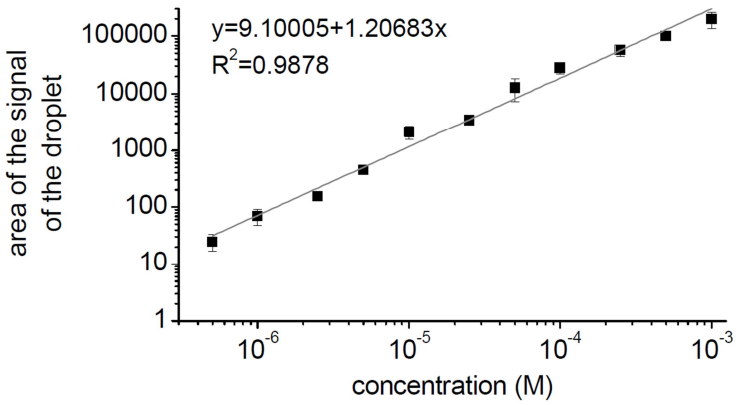

Figure S3: The average signal response of three 10 µL droplets of verapamil at different concentration levels using heat-assisted LAESI shows the linearity of the method. As verapamil was observed as the MH^+ and $[2M+H]^+$ ion at high concentrations, the reported signal was obtained by integrating the areas of the signals, multiplying the area of the signal for the dimer by 2, and adding it to the signal of the MH^+ ion. Note that this approach does not take into account the discrimination of ions at different *m/z*.

a

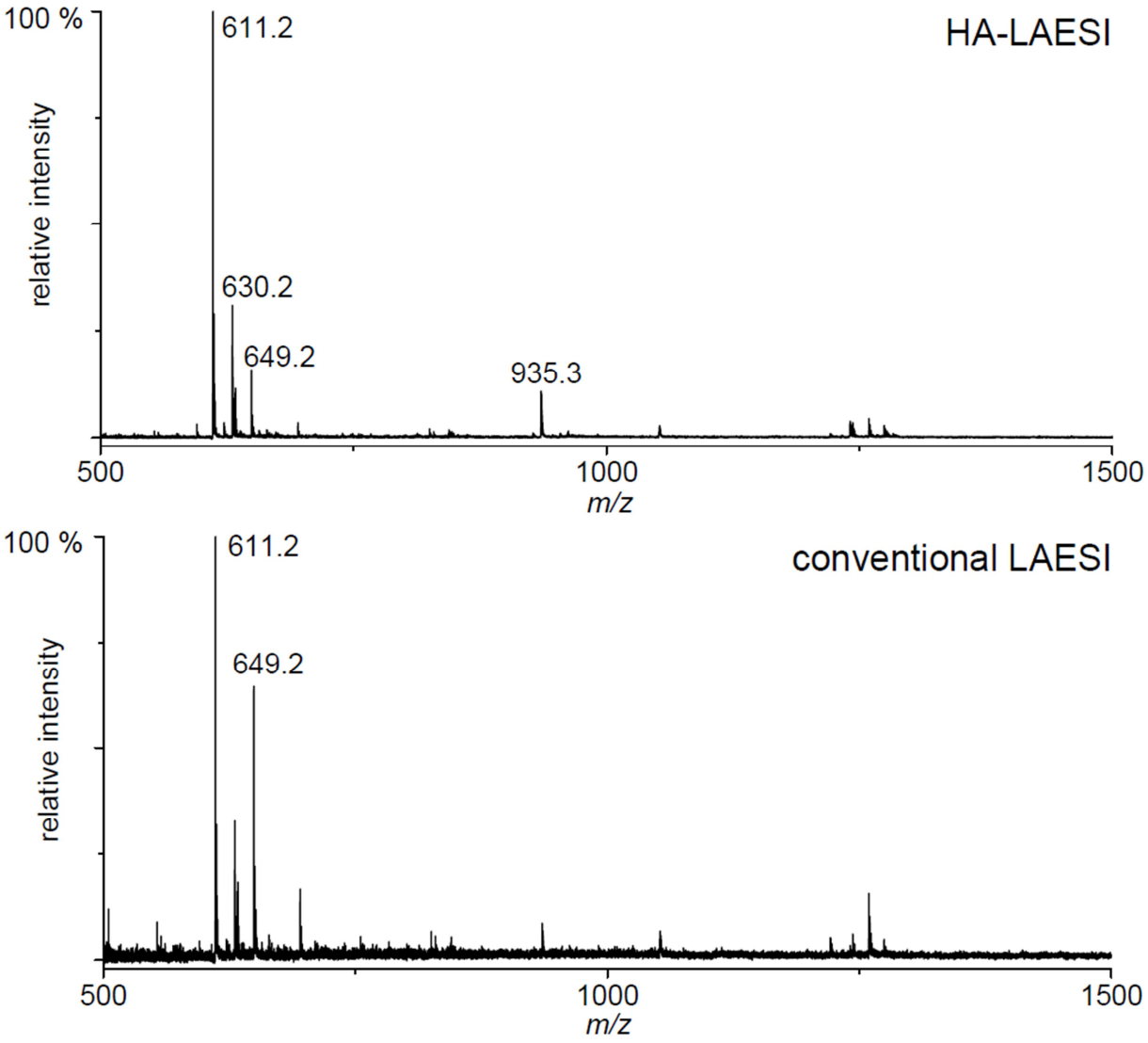
100 %
611.2
HA-LAESI
relative intensity
630.2
649.2
935.3
500
1000
1500
m/z
100 %
611.2
conventional LAESI
649.2
relative intensity
500
1000
1500
m/z

b

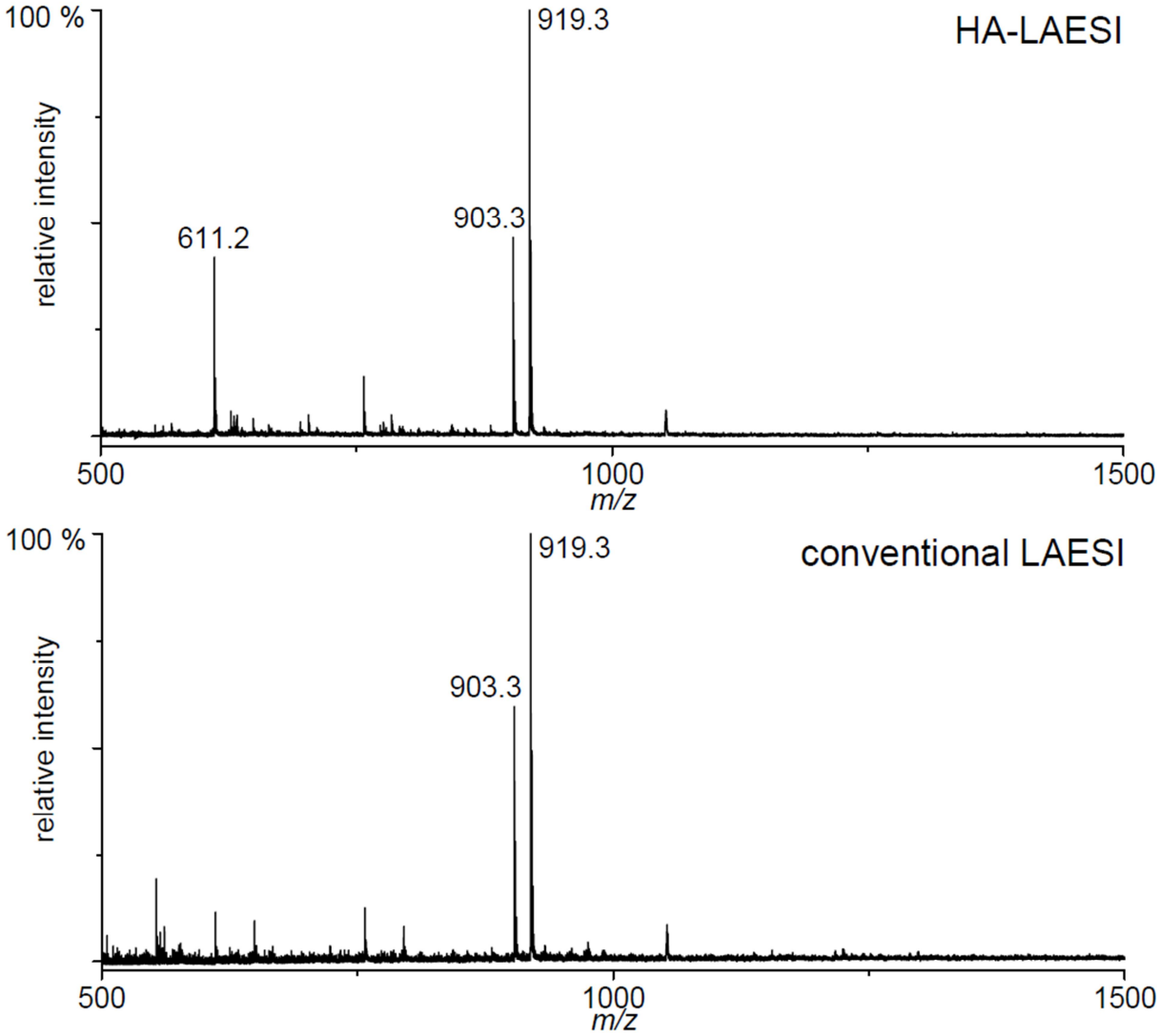

c

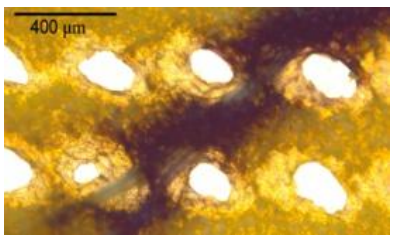

Figure S4: HA-LAESI and conventional LAESI spectra of a) yellow and b) purple tissue of the petal of a pansy. The major ions at 611.2 (yellow tissue), 903.3 (purple tissue), and 919.3 (purple tissue) were thought to correspond to flavonol and anthocyanidin glycosides rutin (quercetin-3-O-rhamnosylglucoside) MH^+, cyanidin-3-p-coumarylrhamnosylglucoside-5-glucoside M^+, and violanin (delphinidin-3-p-coumarylrhamnosylglucoside-5-glucoside) M^+, respectively. c) A microscope image of the petal after ablation.

Table S2: Tentative assignments of selected ions observed from 0.5 mm thick section of the mesocarp of an avocado by HA-LAESI. Spectrum of the tissue is shown in Figure 5a. DG = diglyceride, TG = triglyceride, FA = fatty acyl group. The numbers in parenthesis refer to the total number of fatty acyl carbons and double bonds in the observed ion.

observed *m/z*	compound	ion	calculated *m/z*	Δ*m/z*
313.263	glycerolipids containing 16:0 fatty acid	$[C_{19}H_{37}O_3]^+$	313.274	-0.011
339.277	glycerolipids containing 18:1 fatty acid	$[C_{21}H_{39}O_3]^+$	339.289	-0.012
551.517	DG(32:0)	$[MH-H_2O]^+$	551.503	0.014
	fragment of TG(32:0)	$[MH-FA]^+$	551.503	0.014
577.506	DG(34:1)	$[MH-H_2O]^+$	577.519	-0.013
	fragment of TG(34:1)	$[MH-FA]^+$	577.519	-0.013
595.519	DG (34:1)	MH^+	595.530	-0.011
603.529	DG(36:2)	$[MH-H_2O]^+$	603.535	-0.006
	fragment of TG(36:2)	$[MH-FA]^+$	603.535	-0.006
621.558	DG(36:2)	MH^+	621.545	0.013
638.571	DG(36:2)	$[M+NH_4]^+$	638.572	-0.001
805.736	TG(48:1)	MH^+	805.728	0.008
831.757	TG(50:2)	MH^+	831.744	0.013
833.764	TG(50:1)	MH^+	833.759	0.005
848.773	TG(50:2)	$[M+NH_4]^+$	848.770	0.003
850.783	TG(50:1)	$[M+NH_4]^+$	850.786	-0.003
855.759	TG(52:4)	MH^+	855.744	0.015
	TG(50:1)	$[M+Na]^+$	855.741	0.018
857.760	TG(52:3)	MH^+	857.759	0.001
	TG(50:0)	$[M+Na]^+$	857.757	0.003
	Glucosylceramide (d18:1/26:0)	$[M+NH_4]^+$	857.755	0.005
859.781	TG(52:2)	MH^+	859.775	0.006
	Glucosylceramide (d18:0/26:0)	$[M+NH_4]^+$	859.771	0.010
874.794	TG(52:3)	$[M+NH_4]^+$	874.786	0.008
876.818	TG(52:2)	$[M+NH_4]^+$	876.801	0.017
883.777	TG(54:4)	MH^+	883.775	0.002
	TG(52:1)	$[M+Na]^+$	883.772	0.005
885.793	TG(54:3)	MH^+	885.791	0.002
	TG(52:0)	$[M+Na]^+$	885.788	0.005
887.829	TG(54:2)	MH^+	887.806	0.023
902.837	TG(54:3)	$[M+NH_4]^+$	902.817	0.020

Table S3: Tentative assignments of selected ions observed from 0.5 mm thick section of the mesocarp of an avocado by conventional LAESI. Spectrum of the tissue is shown in Figure 5b. PG= phosphatidyl-glycerol, MGDG = monogalactosyldiglyceride, PE = phosphatidylethanolamine, PC=phophocholine, PA = phosphatidic acid. The numbers in parenthesis refer to the total number of fatty acyl carbons and double bonds in the observed ion.

observed *m/z*	compound	ion	calculated *m/z*	Δ*m/z*
721.515	PG(32:1)	$[M+H]^+$	721.501	0.014
731.539	PE(34:3)	$[M+NH_4]^+$	731.533	0.006
743.528	PC(32:4)	$[M+NH_4]^+$	743.533	-0.005
747.519	PG(34:2)	$[M+H]^+$	747.517	0.002
	MGDG(34:6)	$[M+H]^+$	747.504	0.015
748.502	PC(32:4)	$[M+Na]^+$	748.489	0.013
757.560	PE(36:4)	$[M+NH_4]^+$	757.549	0.011
	PG(36:2)	$[MH-H_2O]^+$	757.538	0.022
	MGDG(34:1)	$[M+H]^+$	757.582	-0.022
759.556	PE(36:3)	$[M+NH_4]^+$	759.565	-0.009
761.572	PE(36:2)	$[M+NH_4]^+$	761.580	-0.008
773.541	PG(36:3)	$[M+H]^+$	773.533	0.008
	PG(34:0)	$[M+Na]^+$	773.530	0.011
	MGDG(36:7)	$[M+H]^+$	773.520	0.021
775.542	PG(36:2)	$[M+H]^+$	775.548	-0.006
	MGDG(36:6)	$[M+H]^+$	775.535	0.007
	PS(34:3)	$[M+NH_4]^+$	775.523	0.019
777.546	MGDG(34:2)	$[M+Na]^+$	777.549	-0.003
	MGDG(36:5)	$[M+H]^+$	777.551	-0.005
	PG(36:1)	$[M+H]^+$	777.564	-0.018
783.572	PE(38:5)	$[M+NH_4]^+$	783.565	0.007
	PA(40:0)	$[M+Na]^+$	783.587	-0.015
	PG(38:3)	$[MH-H_2O]^+$	783.553	0.019
	MGDG(36:2)	$[M+H]^+$	783.598	-0.026
784.596	PC(36:3)	$[M+H]^+$	784.585	0.011
	PC(34:0)	$[M+Na]^+$	784.583	0.013
789.523	PG(34:0)	$[M+K]^+$	789.504	0.019
797.542	PG(38:5)	$[M+H]^+$	797.533	0.009
	PG(36:2)	$[M+Na]^+$	797.530	0.012
	MGDG(36:6)	$[M+Na]^+$	797.517	0.025
799.541	PG(36:1)	$[M+Na]^+$	799.546	-0.005
	PG(38:4)	$[M+H]^+$	799.548	-0.007
	MGDG(36:5)	$[M+Na]^+$	799.533	0.008
801.575	PG(38:3)	$[M+H]^+$	801.564	0.011
	PG(36:0)	$[M+Na]^+$	801.562	0.013
	MGDG(36:4)	$[M+Na]^+$	801.549	0.026

Table S4: Tentative assignments of selected ions observed from 40 μm thick mouse brain tissue section using HA-LAESI. Spectrum of the tissue is shown in Figure 6. DG = diglyceride, TG = triglyceride, FA = fatty acyl group, Cer = ceramide, CE= cholesteryl ester. The numbers in parenthesis refer to the total number of fatty acyl carbons and double bonds in the observed ion.

observed *m/z*	compound	ion	calculated *m/z*	Δ*m/z*
313.278	glycerolipids containing C16:0 fatty acid	$[C_{19}H_{37}O_3]^+$	313.274	0.004
339.291	glycerolipids containing C18:1 fatty acid	$[C_{21}H_{39}O_3]^+$	339.289	0.002
341.302	glycerolipids containing C18:0 fatty acid	$[C_{21}H_{41}O_3]^+$	341.305	-0.003
369.349	cholesterol	$[MH\text{-}H_2O]^+$	369.352	-0.003
548.529	Cer(d18:1/18:0)	$[MH\text{-}H_2O]^+$	548.540	-0.011
551.501	DG(32:0)	$[MH\text{-}H_2O]^+$	551.503	-0.002
	fragment of TG(32:0)	$[MH\text{-}FA]^+$	551.503	-0.002
577.517	DG(34:1)	$[MH\text{-}H_2O]^+$	577.519	-0.002
	fragment of TG(34:1)	$[MH\text{-}FA]^+$	577.519	-0.002
603.540	DG(36:2)	$[MH\text{-}H_2O]^+$	603.535	0.005
	fragment of TG(36:2)	$[MH\text{-}FA]^+$	603.535	0.005
605.554	DG(36:1)	$[MH\text{-}H_2O]^+$	605.550	0.004
	fragment of TG(36:1)	$[MH\text{-}FA]^+$	605.550	0.004
607.571	DG (36:0)	$[MH\text{-}H_2O]^+$	607.566	0.005
	fragment of TG(36:0)	$[MH\text{-}FA]^+$	607.566	0.005
617.520	DG(36:4)	MH^+	617.514	0.006
	DG(34:1)	$[M+Na]^+$	617.512	0.008
623.554	DG(36:1)	MH^+	623.561	-0.007
627.534	DG(38:4)	$[MH\text{-}H_2O]^+$	627.535	-0.001
	fragment of TG(38:4)	$[MH\text{-}FA]^+$	627.535	-0.001
629.543	DG(38:3)	$[MH\text{-}H_2O]^+$	629.550	-0.007
	fragment of TG(38:3)	$[MH\text{-}FA]^+$	629.550	-0.007
630.623	Cer(d18:1/24:1)	$[MH\text{-}H_2O]^+$	630.618	0.005
641.534	DG(38:6)	MH^+	641.514	0.020
	DG(36:3)	$[M+Na]^+$	641.512	0.022
643.551	DG(38:5)	MH^+	643.530	0.021
	DG(36:2)	$[M+Na]^+$	643.527	0.024
645.541	DG(36:1)	$[M+Na]^+$	645.543	-0.002
	DG(38:4)	MH^+	645.545	-0.004

Table S4 continued: Tentative assignments of selected ions observed from 40 μm thick mouse brain tissue section using HA-LAESI. Spectrum of the tissue is shown in Figure 6. DG = diglyceride, TG = triglyceride, FA = fatty acyl group, Cer = ceramide, CE= cholesteryl ester. The numbers in parenthesis refer to the total number of fatty acyl carbons and double bonds in the observed ion.

observed *m/z*	compound	ion	calculated *m/z*	Δ*m/z*
651.545	DG (40:6)	$[MH-H_2O]^+$	651.535	0.010
	fragment of TG (40:6)	$[MH-FA]^+$	651.535	0.010
653.547	DG(40:5)	$[MH-H_2O]^+$	653.550	-0.003
	fragment of TG (40:5)	$[MH-FA]^+$	653.550	-0.003
655.568	DG(40:4)	$[MH-H_2O]^+$	655.566	0.002
	fragment of TG (40:4)	$[MH-FA]^+$	655.566	0.002
667.528	DG(38:4)	$[M+Na]^+$	667.527	0.001
	DG (40:7)	MH^+	667.530	-0.002
669.540	DG(38:3)	$[M+Na]^+$	669.543	-0.003
	DG (40:6)	MH^+	669.545	-0.005
673.572	DG(38:1)	$[M+Na]^+$	673.574	-0.002
	DG(40:4)	MH^+	673.577	-0.005
	CE(18:1)	$[M+Na]^+$	673.589	-0.017
	CE(20:4)	MH^+	673.592	-0.020
686.560	DG(40:6)	$[M+NH_4]^+$	686.572	-0.012
	Cer(d18:1/24:1)	$[M+K]^+$	686.585	-0.025
691.526	DG(40:6)	$[M+Na]^+$	691.527	-0.001
	DG(42:9)	MH^+	691.530	-0.004

CORRESPONDING AUTHORS

*Tiina J. Kauppila
Division of Pharmaceutical Chemistry
Faculty of Pharmacy
P.O. Box 56 (Viikinkaari 5 E)
00014 University of Helsinki
Helsinki, Finland
Tel. +358 9 191 59169
Fax. +358 9 191 59556
E-mail: tiina.kauppila@helsinki.fi

*Akos Vertes
Department of Chemistry
W. M. Keck Institute for Proteomics Technology and Applications
George Washington University
Washington DC 20052
United States
Tel. +1 (202) 994-2717
Fax. +1 (202) 994-5873
E-mail: vertes@gwu.edu